


The Immune Cell Landscape in Renal Allografts

Cell Transplantation
Volume 30: 1–9
© The Author(s) 2021
Article reuse guidelines:
sagepub.com/journals-permissions
DOI: 10.1177/0963689721995458
journals.sagepub.com/home/ccl


Jun Lu^{1,2,*} , Yi Zhang^{1,*}, Jingjing Sun^{1,*}, Shulin Huang³, Weizhen Wu^{1,4}, and Jianming Tan^{1,4}

Abstract

Immune cell infiltration plays an important role in the pathophysiology of kidney grafts, but the composition of immune cells is ill-defined. Here, we aimed at evaluating the levels and composition of infiltrating immune cells in kidney grafts. We used CIBERSORT, an established algorithm, to estimate the proportions of 22 immune cell types based on gene expression profiles. We found that non-rejecting kidney grafts were characteristic with high rates of M2 macrophages and resting mast cells. The proportion of M1 macrophages and activated NK cells were increased in antibody-mediated rejection (ABMR). In T cell-mediated rejection (TCMR), a significant increase in CD8 T cell and $\gamma\delta$ T cell infiltration was observed. CD8 positive T cells were dramatically increased in mixed-ABMR/TCMR. Then, the function of ABMR and TCMR prognostic molecular biomarkers were identified. Finally, we described the gene expression of molecular markers for ABMR diagnosis was elevated and related to the ratio of monocytes and M1 macrophages in ABMR biopsies, while the expression of TCMR diagnosis markers was increased too and positively correlated with $\gamma\delta$ T cells and activated CD4 memory T cells in TCMR biopsies. Our data suggest that CIBERSORT's deconvolution analysis of gene expression data provides valuable information on the composition of immune cells in renal allografts.

Keywords

renal allografts, non-rejecting kidneys, ABMR, TCMR, diagnosis markers

Introduction

Kidney transplantation is the treatment of choice for patients with end-stage renal disease (ESRD)¹. Renal allograft dysfunction may be caused by a variety of causes, including allogeneic immune rejection, viral infection, urinary tract obstruction, calcineurin inhibitor nephrotoxicity, and/or recurrent nephropathy. Based on the immune mechanism, renal transplant rejection is mainly divided into antibody-mediated rejection (ABMR) and T cell-mediated rejection (TCMR)².

ABMR is a major cause of loss of renal allografts³. The diagnosis of ABMR is based on the detection of donor-specific antibodies (DSAs) and significant morphological lesions, significant microcirculatory inflammation, and capillary C4d deposits⁴. Evidence for antibody-mediated damage also include increased NK cell activation⁵ and inflammation-related gene transcripts. Recently, gene expression patterns associated with ABMR have been included in the Banff classification^{6,7}.

TCMR is characterized by interstitial inflammation, tubulitis and intimal arteritis². A large number of studies to date have used immunohistochemical markers to examine

infiltrating cell types. Different cell populations are identified by immunohistochemistry using specific antibodies, such as anti-CD3 antibodies recognizing T cells, anti-CD4 antibodies recognizing helper T cells, anti-CD8 antibodies recognizing cytotoxic T cells, and anti-CD25 antibodies recognizing activated T cells².

¹ Fujian Provincial Key Laboratory of Transplant Biology, Dongfang Hospital (900th Hospital of the Joint Logistics Team), Xiamen University, China

² Laboratory of Basic Medicine, Fuzhou General Clinical College, Fujian Medical University, China

³ University of Liverpool, UK

⁴ Department of Urology, 900th Hospital of the Joint Logistics Team, Fujian, China

* These authors contributed equally to this article

Submitted: June 5, 2020. Revised: January 12, 2021. Accepted: January 28, 2021.

Corresponding Author:

Jun Lu, Fujian Provincial Key Laboratory of Transplant Biology, Xierhuan Road No. 156, Dongfang Hospital (900th Hospital of the Joint Logistics Team), Fuzhou, 350025, China.
Email: junlu.heather@xmu.edu.cn



Traditional histology evaluates the degree of inflammation or tissue damage caused by rejection, usually detected using immunohistochemical markers. This research method can only analyze a small number of immune cell types. Even when tissue immunofluorescence is detected, research is limited by the available fluorescent channels. However, the immune response has many different cell types that coordinate interactions. To accurately study the interaction of immune responses, a large number of analytical samples are required. Recently, a bioinformatics tool, CIBERSORT (cell type identification by estimating relative subsets of known RNA transcripts), was developed⁸. This deconvolution-based tool can use gene expression data to quantify the cellular composition of an immune response. Due to the increasingly recognized advantages of CIBERSORT's algorithm, it has been used to evaluate the composition of immune cells in many cancer types^{9–12}.

In this study, CIBERSORT was used to assess the proportions of 22 immune cells, presenting a comprehensive immune cell landscape in the non-rejecting kidney allografts, ABMR, TCMR, and mixed-ABMR/TCMR. The immune cell composition in TCMR and ABMR may be more deeply understood from the overall immune cell analysis. Moreover, we also explored the links between existing prognostic molecular biomarkers and immune cell infiltration. This analysis method based on genomic detection effectively supplements current studies of immune cell infiltration in organ transplantation using traditional immunohistochemical detection and a small number of gene panels.

Materials and Methods

Data Acquisition

Gene expression profile data were obtained from GEO datasets (GSE98320)¹³. This dataset was obtained by analyzing of the Affymetrix Human Gene Expression Array (GPL15207). Machine learning methods were used to establish a new biopsy diagnostic system. Six archetypes were generated: non-rejecting kidney grafts (NON, $n = 774$), TCMR kidney grafts (TCMR, $n = 81$), three associated with ABMR kidney grafts (ABMR, $n = 326$) (early-stage, fully developed, and late-stage), and mixed-ABMR/TCMR kidney grafts (MIX, $n = 27$). There were no ethical issues. The dataset was normalized using the Limma R package.

Assessment of Immune Infiltration

The CIBERSORT deconvolution algorithm can characterize the cellular composition of complex tissues based on standardized gene expression profiles⁸. This method has been verified by fluorescence-activated cell sorting (FACS). CIBERSORT.R (downloaded from <http://cibersort.stanford.edu/>) was used to examine the relative proportions of 22 invasive immune cell types in each group of kidney grafts. CIBERSORT uses the Leukocyte signature matrix (LM22) signature matrix. LM22 contains 547 genes gene

expression matrix and source data. The CIBERSORT P -value reflects the statistical significance of the deconvolution results for all cell subpopulations. Among all the samples analyzed, we selected 310/299/81/27 of NON / ABMR / TCMR / MIX samples to meet the criterion of CIBERSORT P -value ≤ 0.05 . Immune cell types include: naive B cells, memory B cells, plasma cells, seven T cell types (CD8 + T cells, naive CD4 + T cells, resting memory CD4 + T cells, activated memory CD4 + T cells, T filter Bubble helper cells, Tregs, $\gamma\delta$ T cells), resting natural killer (NK) cells, activated NK cells, monocytes, macrophages (M0 macrophages, M1 macrophages, M2 macrophages), resting-tree dendritic cells (DC), activated DCs, resting mast cells, activated mast cells, eosinophils, and neutrophils.

Gene Expression and Function Analysis

Fold change of the gene expression and the P -value were calculated using the R package limma¹⁴. The gene expression levels of the GSE98320 dataset were visualized using the GraphPad Prism 7 software. Gene Ontology (GO) functional annotation and Kyoto Encyclopedia of Genes and Genomes (KEGG) pathway analyses were conducted through R package clusterProfiler¹⁵ and visualized with the ggplot2 package¹⁶.

Statistical Analysis

Statistical analyses were conducted using R packages. The heatmaps, violin plots, corrplots, and vioplots were generated by R packages and the diagrams were generated using the R language package ggplot2. t -tests were performed to assess the differences in the gene expression of immune checkpoint molecules between various rejecting types of tissues. For all statistical analyses, a P -value < 0.05 was considered significant. The correlation between gene expression level and immune cell infiltration was investigated with Spearman's test.

Results

Immune Cell Infiltration Patterns in Kidney Grafts

The proportions of immune cells in kidney graft were computed on GSE98320, which diagnostic system is established using a machine learning assay. The M2 macrophages in non-rejecting grafts were significantly higher than in other rejecting kidneys ($21.98\% \pm 8.74\%$, $n = 310$, compared with ABMR, $18.11\% \pm 6.12\%$, $n = 299$, $P < 0.001$; TCMR, $18.65\% \pm 7.14\%$, $n = 81$, $P < 0.001$; MIX, $16.97\% \pm 5.62\%$, $n = 27$, $P < 0.001$). Resting mast cells were also increased compared with other rejecting kidneys ($7.03\% \pm 4.02\%$, $n = 310$, compared with ABMR, $5.84\% \pm 2.93\%$, $n = 299$, $P < 0.001$; TCMR, $4.84\% \pm 2.74\%$, $n = 81$, $P < 0.001$; MIX, $3.42\% \pm 2.05\%$, $n = 27$, $P < 0.001$) (Table 1) (Fig. 1A, B).

Table 1. Comparison of CIBERSORT Immune Cell Fractions between Non-Rejecting Kidneys, ABMR, TCMR and Mixed-ABMR/TCMR Biopsies in GSE98320.

Immune cell types	Non-rejecting %	ABMR %	TCMR %	Mixed-ABMR/TCMR %
B cells naive	4.57 ± 3.00	3.57 ± 2.46	3.12 ± 4.11	1.95 ± 2.93
B cells memory	1.16 ± 2.62	0.89 ± 2.39	1.56 ± 2.35	0.75 ± 1.05
Plasma cells	4.31 ± 6.81	3.37 ± 4.63	7.21 ± 9.81	5.24 ± 5.92
T cells CD8	10.97 ± 5.58	12.39 ± 6.12	16.55 ± 8.53	21.76 ± 6.11
T cells CD4 naive	0.37 ± 1.58	0.18 ± 1.01	0.57 ± 1.84	0.12 ± 0.45
T cells CD4 memory resting	4.65 ± 4.89	4.28 ± 4.63	1.13 ± 2.38	0.12 ± 0.66
T cells CD4 memory activated	0.05 ± 0.43	0.08 ± 0.51	1.47 ± 2.46	2.86 ± 4.20
T cells follicular helper	1.53 ± 1.83	1.01 ± 1.45	2.46 ± 2.00	2.89 ± 1.83
T cells regulatory (Tregs)	2.81 ± 2.19	1.93 ± 1.86	1.49 ± 1.68	0.78 ± 0.94
T cells gamma delta	2.40 ± 2.98	4.12 ± 3.78	7.40 ± 3.66	7.50 ± 4.29
NK cells resting	0.02 ± 0.26	0.00 ± 0.00	0.00 ± 0.00	0.00 ± 0.00
NK cells activated	12.01 ± 4.02	13.68 ± 3.22	9.02 ± 3.38	9.27 ± 3.16
Monocytes	4.15 ± 3.94	6.96 ± 5.04	3.68 ± 3.54	5.62 ± 3.28
Macrophages M0	5.38 ± 13.85	0.53 ± 2.76	0.88 ± 1.97	0.57 ± 1.75
Macrophages M1	14.78 ± 7.01	21.11 ± 5.67	18.40 ± 5.63	19.17 ± 4.86
Macrophages M2	21.98 ± 8.74	18.11 ± 6.12	18.65 ± 7.14	16.97 ± 5.62
Dendritic cells resting	1.19 ± 1.34	1.29 ± 1.53	0.64 ± 0.92	0.40 ± 0.70
Dendritic cells activated	0.05 ± 0.31	0.19 ± 0.62	0.08 ± 0.25	0.08 ± 0.20
Mast cells resting	7.03 ± 4.02	5.84 ± 2.93	4.84 ± 2.74	3.42 ± 2.05
Mast cells activated	0.10 ± 0.84	0.05 ± 0.50	0.01 ± 0.10	0.00 ± 0.00
Eosinophils	0.21 ± 0.67	0.23 ± 0.76	0.71 ± 1.34	0.45 ± 0.70
Neutrophils	0.24 ± 1.99	0.19 ± 1.58	0.12 ± 0.64	0.06 ± 0.21

Compared with non-rejecting kidneys (14.78% ± 7.01%, $n = 310$), the M1 macrophages in ABMR tissues were significantly elevated (21.11% ± 5.67%, $n = 299$, $P < 0.001$). The number of activated NK cells in ABMR were increased (13.68% ± 3.22%, $n = 299$, compared with 12.01% ± 4.02% in non-rejecting kidneys, $n = 310$, $P < 0.001$). In addition, monocytes increased in ABMR (6.96% ± 5.04%, $n = 299$, compared with 4.15% ± 3.94% in non-rejecting kidneys, $n = 310$, $P < 0.001$) (Table 1) (Fig. 1A, B). There were three sub-phenotypes in ABMR (early stage-(EABMR), fully developed-(FABMR), late stage-(LABMR)). As we showed in Supplemental Table S1, the proportion of activated NK cells in the three sub-phenotypes is higher than that of non-rejecting kidneys, and the difference between the three sub-phenotypes is small. The ratio of M1 macrophages is more consistent in EABMR and FABMR. These results indicate that the increased ratio of activated NK cells and M1 macrophages is a common feature of ABMR.

T cell activation is the main feature of TCMR. Compared with non-rejecting kidneys (22.79% ± 4.76%, $n = 310$) and ABMR (22.95% ± 5.92%, $n = 299$), the total percentage of T cells was significantly increased in TCMR (31.08% ± 6.66%, $n = 81$, $P < 0.001$). The proportion of CD8 T cells increased (16.55% ± 8.53%, $n = 81$, compared with non-rejecting kidneys 10.97% ± 5.58%, $n = 310$, $P < 0.001$ or ABMR 12.39% ± 6.12%, $n = 299$, $P < 0.001$). $\gamma\delta$ T cells were also strongly increased in TCMR (7.40% ± 3.66%, $n = 81$, compared with 2.40% ± 2.98% of non-rejecting kidneys, $n = 310$, $P < 0.001$ or ABMR 4.12% ± 3.78%, $n = 299$, $P < 0.001$).

In the GSE98320 dataset, the proportion of immune cells in the mixed-ABMR/TCMR group is more similar to that of the TCMR group, especially the T cell sub-types. CD8 T cells were extremely increased in mixed-ABMR/TCMR compared with other group (21.76% ± 6.11%, $n = 27$, compared with non-rejecting kidneys, 10.97% ± 5.58%, $n = 310$, $P < 0.001$; ABMR, 12.39% ± 6.12%, $n = 299$, $P < 0.001$; TCMR, 16.55% ± 8.53%, $n = 81$, $P < 0.001$) (Table 1) (Fig. 1A, B).

CD45, a gene commonly expressed in lymphocytes. The expression analysis result of CD45 in the non-rejecting kidney allografts, ABMR, TCMR, and mixed-ABMR/TCMR was showed in Supplemental Figure S1. Compared with non-rejecting kidneys, the expression of CD45 was elevated in three rejection groups, indicating that the overall proportion of lymphocytes may increase.

The Function of Diagnostic and Prognostic Molecular Biomarkers of ABMR and TCMR

At the Banff meeting in 2015 and 2017, a summary of opinions was obtained indicating a strong link between Banff histological lesions in some molecular markers^{6,7}. As a diagnostic classifier, the expression equations of these genes are summarized by quantifying the respective genes or by weighting. In 2017, Banff gave a total of 103 genes in the four ABMR gene pools⁷ (Supplemental Table S1). The GO and KEGG pathway annotations were used to predict the function of these genes. Multiple GO and KEGG pathway annotations were obtained when the P -value was less than 0.01. Multiple pathways involved

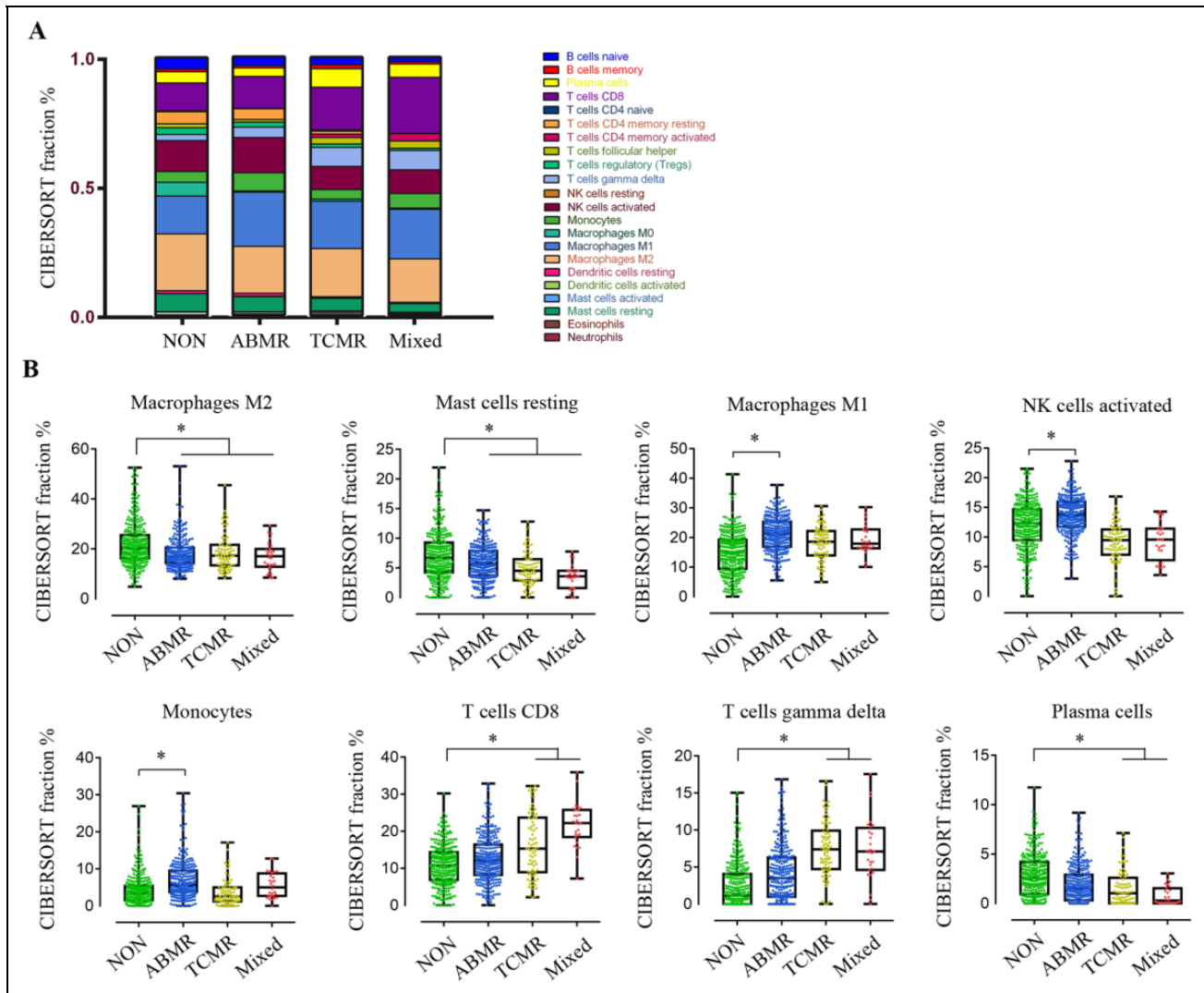


Figure 1. Analysis of immune cell distribution in kidney grafts through a GEO dataset (GSE98320). (A) The CIBERSORT algorithm was applied to the transcriptomic data of the GSE98320 samples. The averaged relative distribution of 22 leukocyte types was compared by type of rejection (see also Table 1). (B) Macrophages M2, mast cells resting, macrophages M1, NK cells activated, monocyte, T cells CD8, T cells gamma delta ($\gamma\delta$ T), and plasma cell infiltration were estimated. * $P < 0.001$.

mechanisms of chronic inflammation formation, such as CXCL chemokine receptor binding, cytokine-cytokine receptor interaction, and TNF signaling pathways (Fig. 2A, B).

There are 69 genes in the four TCMR gene pools given by Banff 2017 (Haas et al., 2018). The GO and KEGG pathway annotations were used to predict the functions of these genes. Multiple GO and KEGG pathway annotations were obtained at P -values < 0.01 , and multiple pathways involved T cell activation, such as T cell receptor signaling pathways, cell adhesion molecules (CAMs), and Th17 cell differentiation (Fig. 2C, D).

Associations between Immune Cell Infiltration and Transcriptomic Features

Fifteen of the genes used for ABMR diagnosis were present in three ABMR gene pools (Fig. 3A), except that one gene

(DARC) had a very low abundance of expression. The expression of the other 14 genes was higher in the ABMR group than in the non-rejection group of GSE98320 (Fig. 3B) (Supplemental Table S2). The analysis of the correlation between the expression of these 14 genes and the ratio of ABMR immune cells showed that most of the genes were strongly correlated with M1 macrophages and monocytes cells (Fig. 3C). Seventeen of the genes used for TCMR diagnosis were present in three pools of TCMR genes (Fig. 3D) (Supplemental Table S3). These 17 genes were highly expressed in the TCMR group of GSE98320 (Fig. 3E) (Supplemental Table S4). Analysis of the correlation between the expression of these 17 genes and the ratio of immune cells revealed that they were strongly associated with $\gamma\delta$ T cells and activated CD4 memory T cells (Fig. 3F). The results of these analyses indicate that the marker molecules used in the current rejection diagnosis are all key

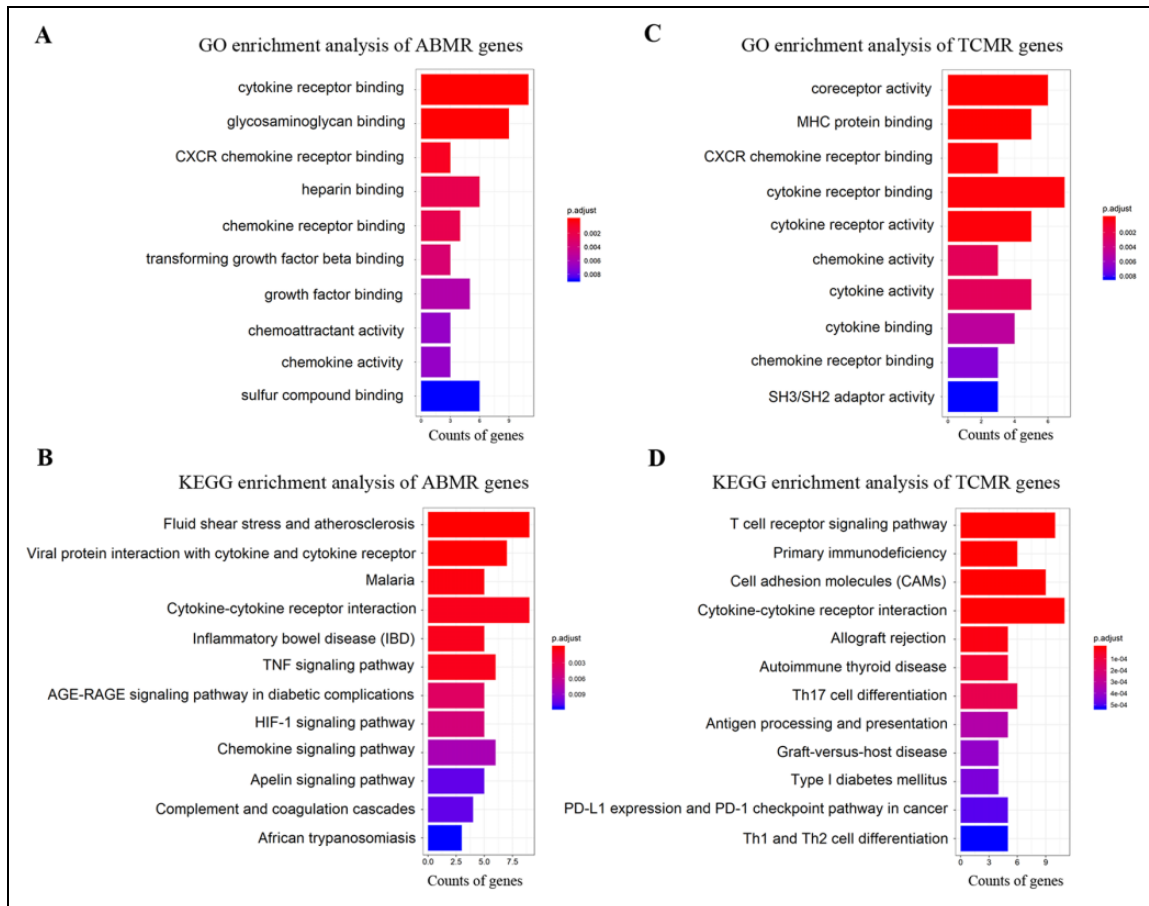


Figure 2. Functional annotation of ABMR and TCMR transcripts. (A) Enrichment analysis of gene ontology (GO) ABMR molecular biomarkers. The x-axis represents the number of genes in each GO term. (B) KEGG pathway annotations of the ABMR molecular biomarkers. The x-axis shows the number of genes annotated. (C) Enrichment analysis of gene ontology (GO) TCMR molecular biomarkers. The x-axis represents the number of genes in each GO term. (D) KEGG pathway annotations of the TCMR molecular biomarkers. The x-axis shows the number of genes annotated.

molecules in the immune response. Their expression was positively correlated with the immune cell infiltration characteristics of each type of rejection analyzed by CIBERSORT.

Taking the correlation analysis between CX3CR1 gene expression and immune cell infiltration ratio in ABMR as an example, it can be seen that the expression of CX3CR1 was strongly correlated with the infiltration ratio of monocytes and M1 macrophages in ABMR biopsies, with correlation coefficients of 0.41 and 0.32, ($P < 0.001$) (Fig. 4A, B). In TCMR, using SH2D1A as an example, the correlation analysis between SH2D1A gene expression and immune cell infiltration ratio in TCMR showed that the expression of SH2D1A was strongly correlated with the ratio of $\gamma\delta$ T cells and CD4 memory T cells, with correlation coefficients of 0.70 and 0.55, respectively ($P < 0.001$) (Fig. 4C, D).

Discussion

In this study, we performed a detailed evaluation of immune cell infiltration in renal tissue after kidney transplantation based on CIBERSORT deconvolution of large amounts of

gene expression data from a large number of samples. We observed differences in immune cell composition in the non-rejection group and the major subtypes of rejection.

Here, in the non-rejection group study, we found a specific elevation of M2 macrophages and resting mast cells. It is hypothesized that M2 macrophages and mast cells at rest play an important role in maintaining the immune balance of the graft. Previous studies have found that mast cells strive to maintain tissue homeostasis under “resting conditions”¹⁷. Mast cells continue to communicate with the microenvironment through two secretory mechanisms, fractional degranulation (PMD) and exosome release. These extracellular vesicles are complex messengers that have immunomodulatory functions on T and B lymphocytes¹⁸ and dendritic cells¹⁹.

In ABMR we observed an increase in the proportion of M1 macrophages, monocytes and activated NK cells. The increase in the number of NK cells is an important breakthrough in the study of ABMR in recent years^{5,20,21}. NK cell induction is the main feature of ABMR after kidney and heart transplantation²². The importance of NK cells in

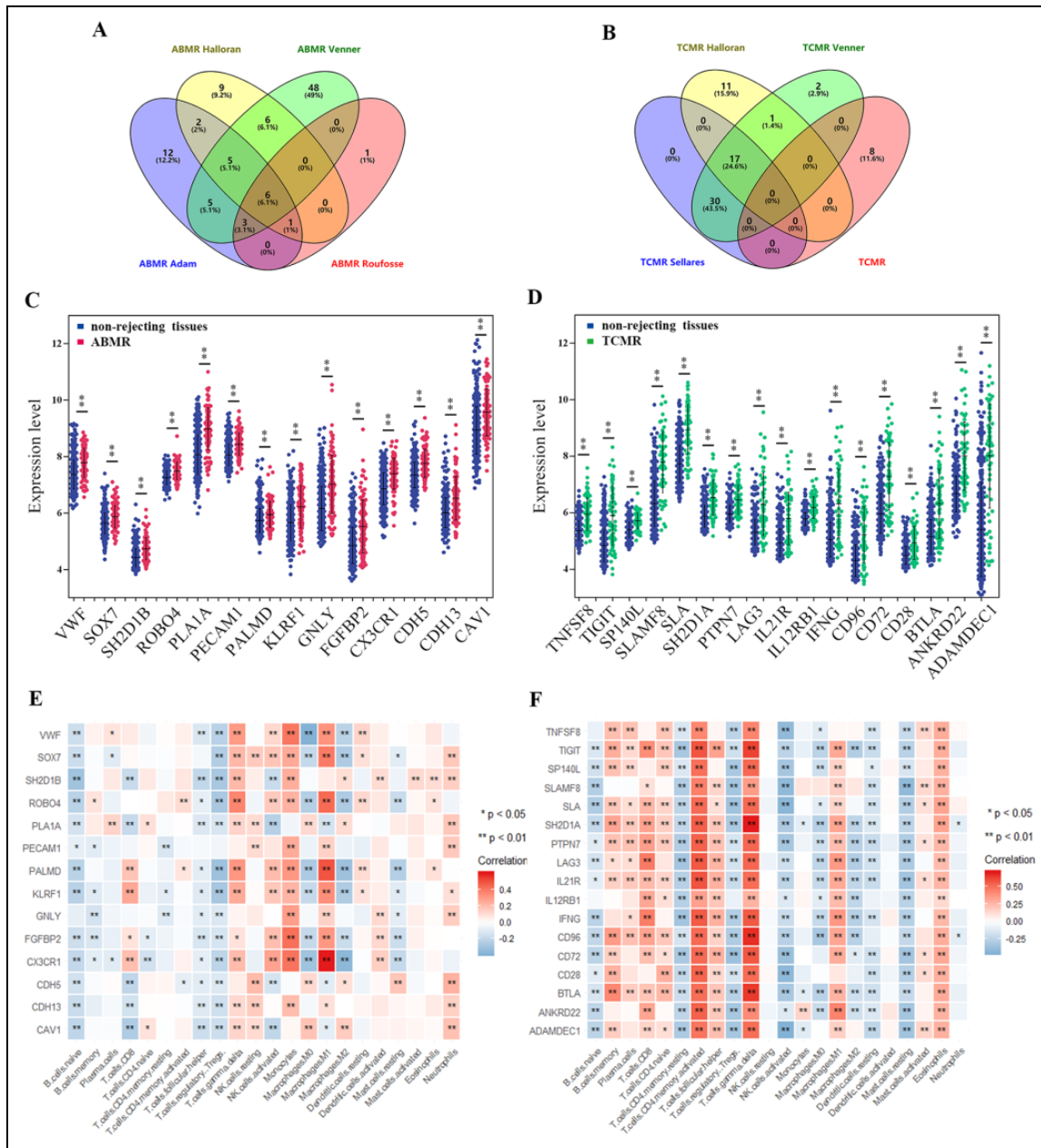


Figure 3. The correlation between gene sets and immune cell infiltration ratio. (A) Venn diagram of intersections of the four ABMR gene sets. (B) The relative gene expression levels of 14 genes in ABMR and non-rejecting biopsies. (C) Correlation analysis between the expression of 14 genes and the ratio of immune cell infiltration in ABMR. (D) Venn diagram of intersections of the four TCMR gene sets. (E) The relative gene expression levels of 17 genes in TCMR and non-rejecting biopsies. (F) Correlation analysis between the expression of 17 genes and the ratio of immune cell infiltration in TCMR. A red box indicates a positive correlation, blue negative, and P -values were corrected for false discovery rate. * P -value < 0.05, ** P -value < 0.01.

ABMR is supported by animal studies^{23–25}. NK cells are primarily involved in complement-independent rejection mechanisms such as antibody-dependent cellular cytotoxicity (ADCC)²¹.

In TCMR, we observed a significant increase in the total number of T cells and a significant increase in CD8 T cells and $\gamma\delta$ T cells. Although the role of $\gamma\delta$ T in transplanted kidney is controversial²⁶, there are also reports that $\gamma\delta$ T cells perform multiple effector functions, including

cytotoxic activity and production of the pro-inflammatory cytokine interleukin (IL)-17A²⁷. Of course, the author cannot rule out the error of the CIBERSORT algorithm in calculating $\gamma\delta$ T. In addition, with the advent of single cell RNA sequencing, it would be valuable to confirm our data with actual single cell data.

The latest revision of the Banff classification encourages the use of molecular markers as an alternative diagnostic criterion for transplant rejection. Multiple gene sets are

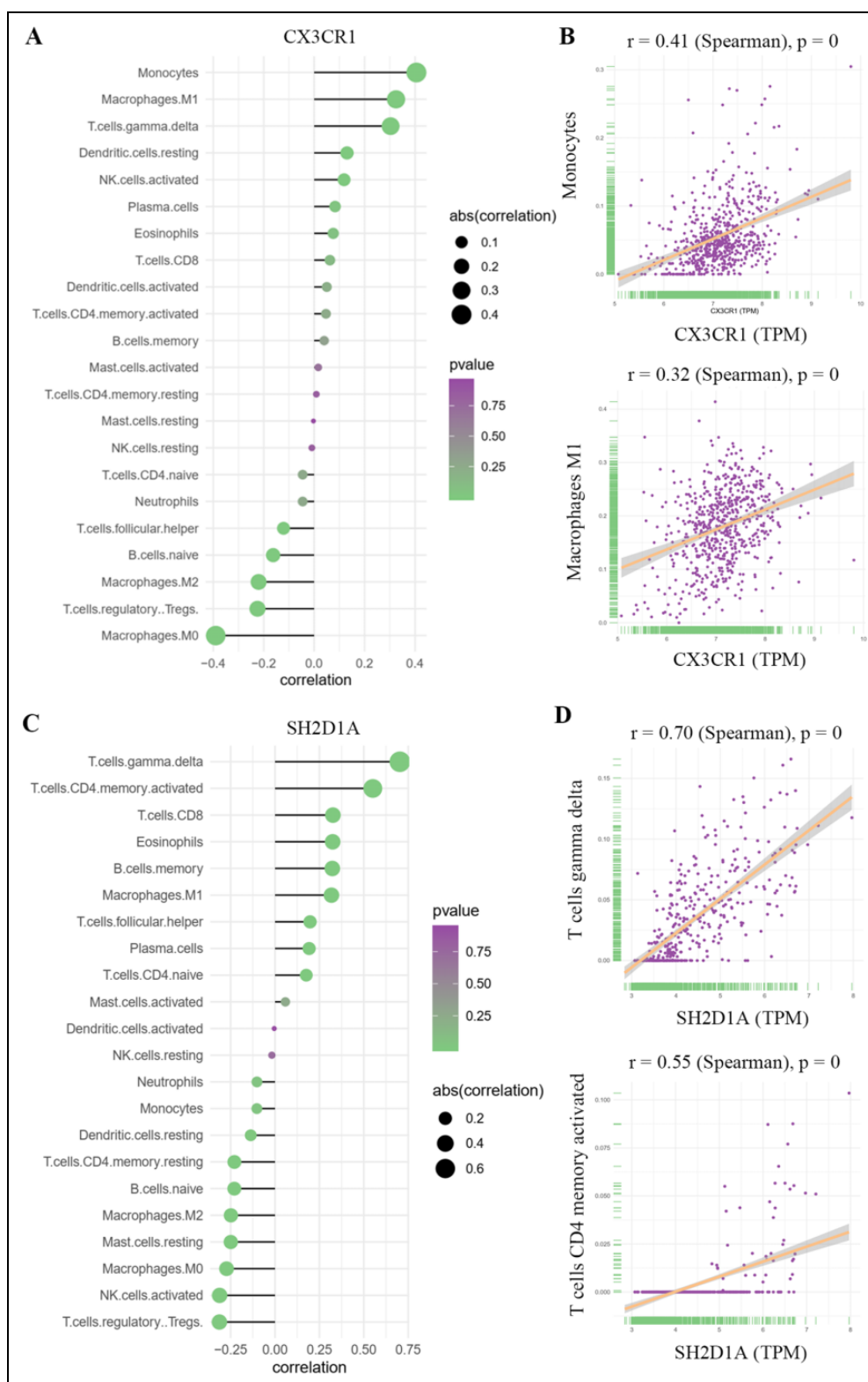


Figure 4. The correlation between CX3CR1 or SH2D1A gene expression and immune cell infiltration ratio. (A) Lollipop plot of correlation between CX3CR1 gene expression and 22 immune cell infiltration ratios in ABMR. The size of the ball represents the strength of correlation estimated by Spearman correlation analysis. (B) Scatter plot of CX3CR1 expression vs. ABMR immune cell infiltration ratios of monocytes and macrophages M1. (C) Lollipop plot of correlation between SH2D1A gene expression and 22 immune cell infiltration ratios in TCMR. The size of the ball represents the strength of correlation estimated by Spearman correlation analysis. (D) Scatter plot of SH2D1A expression vs. TCMR immune cell infiltration ratios of T cells gamma delta ($\gamma\delta$ T cells) and T cells CD4 memory activated.

given for different types of rejection^{6,7}. In our study, we found that the molecular markers of ABMR and TCMR were highly expressed in the respective exclusion groups. We also analyzed the correlations between gene expression and immune cell infiltration ratio and found that important molecular markers for ABMR diagnosis are related to the ratio of M1 macrophages and monocytes. Although the 14 ABMR diagnosing molecular markers we analyzed did not show correlations with NK cell infiltration, the ABMR Venner gene set, which contains a large number of genes, contained genes that respond to NK cell activation. Molecular markers for TCMR diagnosis have a positive correlation with $\gamma\delta$ T cells and activated CD4 memory T cells.

Traditional pathological histochemistry remains the primary method for diagnosing graft rejection. Although the type of rejection cannot be clearly distinguished by the proportion of 22 immune cell infiltrations, gene expression profiles based on gene chips and RNA sequences can be used to assess immune cell ratios by CIBERSORT, as well as to obtain immune-related genes recommended in all Banff standards, indicating that gene expression profiling greatly complements traditional pathological analysis. The detection of gene expression and the calculation of the ratio of immune cells allow us to fully understand the immune status of renal allografts in patients.

Here, we describe in detail the pattern of immune infiltration in different types of kidney allografts with or without rejection. The relationship between the diagnostic molecular markers and the immune infiltration pattern is further established. Our work promotes the study of the immune response in kidney grafts after transplantation.

Acknowledgments

The authors are grateful to the GEO database for providing high-quality data.

Authors Contributions

J.L. designed the experiments. J.L., Y.Z., J.J.S., S.L.H., W.Z.W., and J.M.T. analyzed the data. J.L. wrote the manuscript.

Ethical Approval

All data were obtained from GEO datasets, so there were no ethical issues.

Statement of Human and Animal Rights

This article does not contain any studies with human or animal subjects.

Statement of Informed Consent

There are no human subjects in this article and informed consent is not applicable.


Declaration of Conflicting Interests

The author(s) declared no potential conflicts of interest with respect to the research, authorship, and/or publication of this article.

Funding

The author(s) disclosed receipt of the following financial support for the research, authorship, and/or publication of this article: This work was supported by the National Key Clinical Specialty Army Construction Project of China (2013LZ001), Science and Technology Innovation Joint Fund of Fujian Province (grant numbers: 2018Y9115), Natural Science Foundation of Fujian Province (grant numbers: 2018J01345 and 2019J01528), National Natural Science Foundation of China (grant numbers: 81870515) and Outstanding Youth Funds of the 900 Hospital of the Joint Logistics Team (grant numbers: 2017Q07).

ORCID iD

Jun Lu  <https://orcid.org/0000-0003-2221-1872>

Supplemental Material

Supplemental material for this article is available online.

References

1. Locatelli F, Pozzoni P, Del Vecchio L. Renal replacement therapy in patients with diabetes and end-stage renal disease. *J Am Soc Nephrol.* 2004;15(Suppl 1):S25–S29.
2. Kanzaki G, Shimizu A. Currently available useful immunohistochemical markers of renal pathology for the diagnosis of renal allograft rejection. *Nephrology (Carlton).* 2015;20(Suppl 2):9–15.
3. Einecke G, Sis B, Reeve J, Mengel M, Campbell PM, Hidalgo LG, Kaplan B, Halloran PF. Antibody-mediated microcirculation injury is the major cause of late kidney transplant failure. *Am J Transplant.* 2009;9(11):2520–2531.
4. Solez K, Colvin RB, Racusen LC, Haas M, Sis B, Mengel M, Halloran PF, Baldwin W, Banfi G, Collins AB, Cosio F, et al. Banff 07 classification of renal allograft pathology: updates and future directions. *Am J Transplant.* 2008;8(4):753–760.
5. Hidalgo LG, Sis B, Sellares J, Campbell PM, Mengel M, Einecke G, Chang J, Halloran PF. NK cell transcripts and NK cells in kidney biopsies from patients with donor-specific antibodies: evidence for NK cell involvement in antibody-mediated rejection. *Am J Transplant.* 2010;10(8):1812–1822.
6. Loupy A, Haas M, Solez K, Racusen L, Glotz D, Seron D, Nankivell BJ, Colvin RB, Afrouzian M, Akalin E, Alachkar N, et al. The Banff 2015 kidney meeting report: current challenges in rejection classification and prospects for adopting molecular pathology. *Am J Transplant.* 2017;17(1):28–41.
7. Haas M, Loupy A, Lefaucheur C, Roufosse C, Glotz D, Seron D, Nankivell BJ, Halloran PF, Colvin RB, Akalin E, Alachkar N, et al. The Banff 2017 kidney meeting report: revised diagnostic criteria for chronic active T cell-mediated rejection, antibody-mediated rejection, and prospects for integrative endpoints for next-generation clinical trials. *Am J Transplant.* 2018;18(2):293–307.
8. Newman AM, Liu CL, Green MR, Gentles AJ, Feng W, Xu Y, Hoang CD, Diehn M, Alizadeh AA. Robust enumeration of cell subsets from tissue expression profiles. *Nat Methods.* 2015;12(5):453–457.

9. Zhang S, Zhang E, Long J, Hu Z, Peng J, Liu L, Tang F, Li L, Ouyang Y, Zeng Z. Immune infiltration in renal cell carcinoma. *Cancer Sci.* 2019;110(5):1564–1572.
10. Rohr-Udilova N, Klinglmueller F, Schulte-Hermann R, Stift J, Herac M, Salzmann M, Finotello F, Timelthaler G, Oberhuber G, Pinter M, Reiberger T, et al. Deviations of the immune cell landscape between healthy liver and hepatocellular carcinoma. *Sci Rep.* 2018;8(1):6220.
11. Zhou R, Zhang J, Zeng D, Sun H, Rong X, Shi M, Bin J, Liao Y, Liao W. Immune cell infiltration as a biomarker for the diagnosis and prognosis of stage I-III colon cancer. *Cancer Immunol Immunother.* 2019;68(3):433–442.
12. Zhou L, Xu L, Chen L, Fu Q, Liu Z, Chang Y, Lin Z, Xu J. Tumor-infiltrating neutrophils predict benefit from adjuvant chemotherapy in patients with muscle invasive bladder cancer. *Oncoimmunology.* 2017;6(4):e1293211.
13. Reeve J, Bohmig GA, Eskandary F, Einecke G, Lefaucheur C, Loupy A, Halloran PF, group MM-Ks. Assessing rejection-related disease in kidney transplant biopsies based on archetypal analysis of molecular phenotypes. *JCI Insight.* 2017;2(12):e94197.
14. Ritchie ME, Phipson B, Wu D, Hu Y, Law CW, Shi W, Smyth GK. limma powers differential expression analyses for RNA-sequencing and microarray studies. *Nucleic Acids Res.* 2015;43(7):e47.
15. Yu G, Wang LG, Han Y, He QY. clusterProfiler: an R package for comparing biological themes among gene clusters. *OMICS.* 2012;16(5):284–287.
16. Ito K, Murphy D. Application of ggplot2 to Pharmacometric Graphics. *CPT Pharmacometrics Syst Pharmacol.* 2013;2(10):e79.
17. Frossi B, Mion F, Tripodo C, Colombo MP, Pucillo CE. Rheostatic functions of mast cells in the control of innate and adaptive immune responses. *Trends Immunol.* 2017;38(9):648–656.
18. Skokos D, Le Panse S, Villa I, Rousselle JC, Peronet R, David B, Namane A, Mecheri S. Mast cell-dependent B and T lymphocyte activation is mediated by the secretion of immunologically active exosomes. *J Immunol.* 2001;166(2):868–876.
19. Skokos D, Botros HG, Demeure C, Morin J, Peronet R, Birkenmeier G, Boudaly S, Mecheri S. Mast cell-derived exosomes induce phenotypic and functional maturation of dendritic cells and elicit specific immune responses *in vivo*. *J Immunol.* 2003;170(6):3037–3045.
20. Parkes MD, Halloran PF, Hidalgo LG. Mechanistic sharing between NK cells in ABMR and effector T cells in TCMR. *Am J Transplant.* 2018;18(1):63–73.
21. Yazdani S, Callemeyn J, Gazut S, Lerut E, de Looor H, Wevers M, Heylen L, Saison C, Koenig A, Thauinat O, Thorrez L, et al. Natural killer cell infiltration is discriminative for antibody-mediated rejection and predicts outcome after kidney transplantation. *Kidney Int.* 2019;95(1):188–198.
22. Loupy A, Duong Van Huyen JP, Hidalgo L, Reeve J, Racape M, Aubert O, Venner JM, Falmuski K, Bories MC, Beuscart T, Guillemain R, et al. Gene expression profiling for the identification and classification of antibody-mediated heart rejection. *Circulation.* 2017;135(10):917–935.
23. Hidalgo LG, Sellares J, Sis B, Mengel M, Chang J, Halloran PF. Interpreting NK cell transcripts versus T cell transcripts in renal transplant biopsies. *Am J Transplant.* 2012;12(5):1180–1191.
24. Hirohashi T, Chase CM, Della Pelle P, Sebastian D, Alessandrini A, Madsen JC, Russell PS, Colvin RB. A novel pathway of chronic allograft rejection mediated by NK cells and alloantibody. *Am J Transplant.* 2012;12(2):313–321.
25. Kohei N, Tanaka T, Tanabe K, Masumori N, Dvorina N, Valujskikh A, Baldwin WM, 3rd, Fairchild RL. Natural killer cells play a critical role in mediating inflammation and graft failure during antibody-mediated rejection of kidney allografts. *Kidney Int.* 2016;89(6):1293–1306.
26. Puig-Pey I, Bohne F, Benitez C, Lopez M, Martinez-Llordella M, Oppenheimer F, Lozano JJ, Gonzalez-Abraldes J, Tisone G, Rimola A, Sanchez-Fueyo A. Characterization of gamma delta T cell subsets in organ transplantation. *Transpl Int.* 2010;23(10):1045–1055.
27. Locatelli F, Pozzoni P, Del VL. Renal replacement therapy in patients with diabetes and end-stage renal disease. *J Am Soc Nephrol.* 2004;15(Suppl 1):S25–S29.